Influence of cavitation on atomisation at low pressures using up-scaled and transparent nozzles

R. Ochoterena*, P. Li, M. Vera-Hernández, and S. Andersson
Department of Applied Mechanics
Chalmers University of Technology
SE-41296, Göteborg Sweden

Abstract

The influence of cavitation on atomisation was studied using up-scaled, optically transparent nozzles, injecting water at four different temperatures into air at ambient conditions. The flow inside the nozzle and atomisation were related using the length of the cavitation length and cone angle as main experimental parameters. Results from these experiments, where the effects of the aerodynamic forces are small compared to the internal flow effects, show that the same length of cavitation leads to a similar degree of atomisation regardless of the pressure drop across the nozzle, fluid temperature or flow velocity inside the nozzle.

Introduction

Cavitation and turbulence play important roles in atomisation and spray behaviour [1, 2]. However, the individual contribution from each of them, neither from turbulence nor from cavitation, has been clearly understood yet [3–5]. The difficulty of defining the individual contribution of each of the former phenomena on atomisation resides mainly in the arduousness of isolating cavitation from turbulence or vice versa due to the fact that cavitation appears at high flow rates where turbulence is generally present too. A further difficulty arises from the fact that turbulence also affects the inception of cavitation due to the fact that cavitation nuclei can be located in the core of vortices where the local pressure is lower than the average pressure inside the nozzle [6, 7].

Water vapour pressure is temperature dependent and, in principle, it is possible to promote the appearance of cavitation inside the nozzle, over turbulence, by modifying the temperature of the working fluid [8]. Based on this, the individual influence of cavitation on atomisation can be investigated injecting water at different and controlled temperatures into air at ambient conditions using, up-scaled, optically transparent nozzles.

The purpose of this work was to study the solely influence of cavitation on atomisation in cases where atomisation is strongly influenced by flow effects inside the nozzle and weakly influenced by aerodynamical forces. Achieving this by injecting water at temperatures above the ambient temperature into ambient air trough optically accesible nozzles.

The employed nozzles are optically transparent and have a round cross section throughout. Both nozzles differ between them in the smoothness of the border of the contraction zone. One has a sharp inlet and the other has a blunt or smooth inlet. Atomisation was related to cavitation using the spray cone angle and the cavitation length, i.e. the distance from the nozzle inlet to the farthest downstream border of cavitation, respectively, as main experimental parameters.

Experimental set-up

The experimental set-up consists of optical transparent nozzles, one with a sharp inlet and the other with a rounded inlet, and a rig that injects water at controlled pressures and temperatures into ambient air. The test rig is equipped with a pump, a settling chamber to reduce turbulence upstream the nozzle, a 500 litre insulated reservoir with a heating element of 18 kW, a transparent observation chamber downstream the nozzle, and a pressure transducer at the nozzle inlet. Figure 1 depicts the experimental set-up used for this study.

The investigated nozzles were manufactured of a transparent polymer and have a circular cross section throughout. The nozzles have a geometrical difference between them at the inlet of the contraction zone; one has a sharp inlet border (Figure 2(b)) while the other nozzle has a blunt border inlet (Figure 2(a)). This geometrical difference between these nozzles leads to the consequence that the sharp inlet nozzle produces an atomising spray while the blunt inlet nozzle produces a non-atomising jet. The nozzles and their dimensions are depicted on Figure 2.

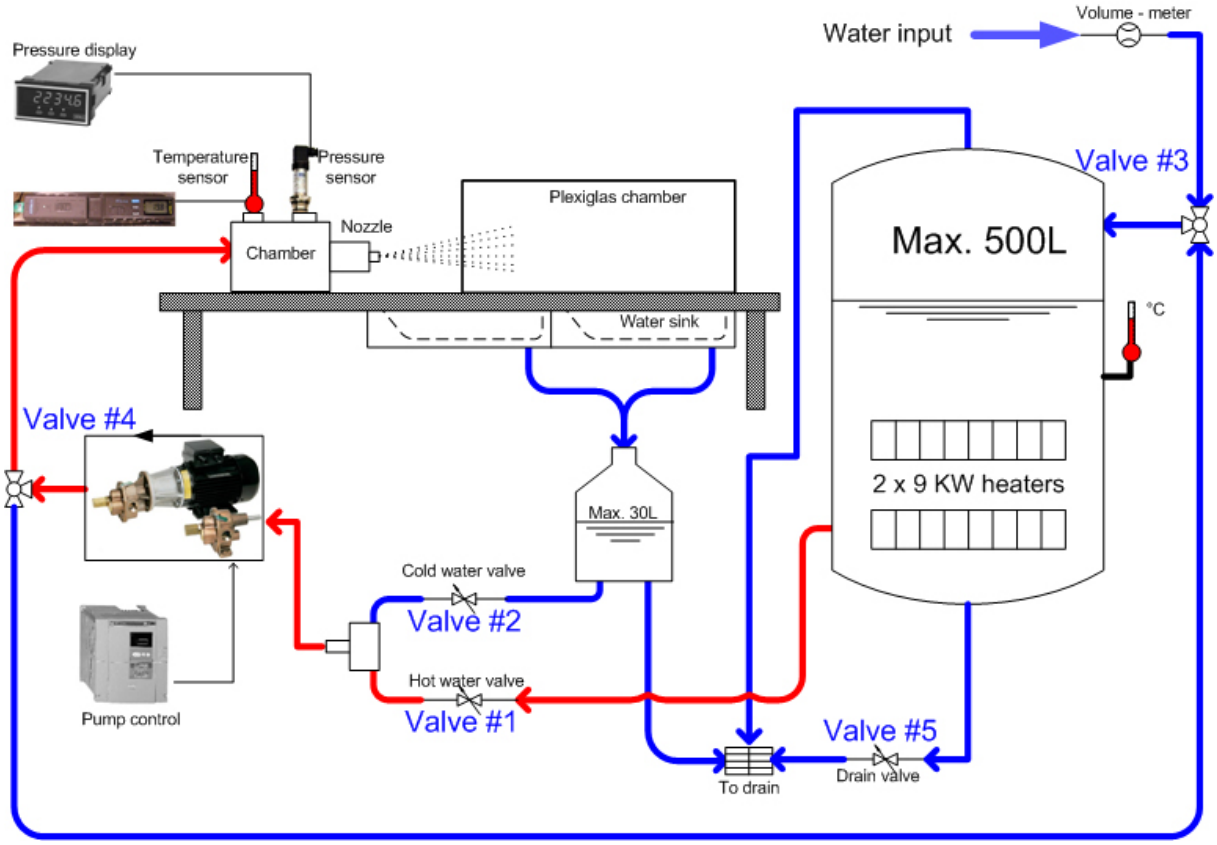

Figure 1. Sketch of the experimental set-up showing its main components: Isolated and heated water reservoir, positive displacement pump, pump control, temperature sensor, settling chamber, pressure transducer, nozzle and observation section.

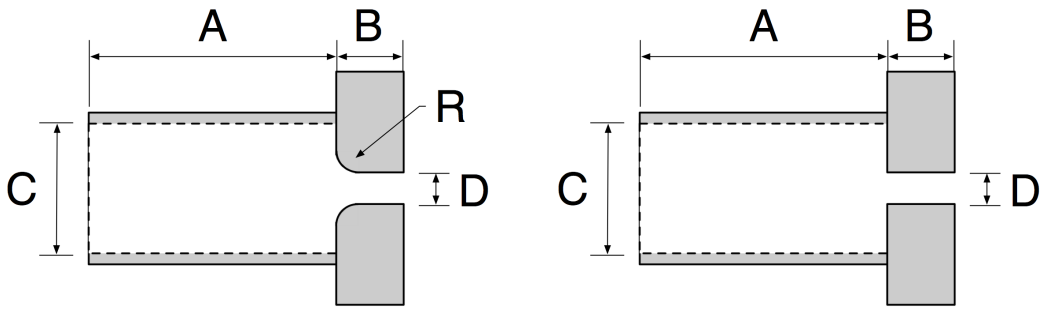

(a) Blunt inlet nozzle (b) Sharp inlet nozzle

Figure 2. Drawings at a middle cut of the studied nozzles. A=6D, B=3D, C=4D, D=5mm, R=0.5mm (blunt nozzle only).

Experimental procedure

Water properties, in the temperature range studied under this work, such as density (ρ), surface tension (γ), dynamic viscosity (μ) and vapour pressure (P_v) are shown in Table 1.

The experimental matrix is presented in Figure 3. The test matrix relates fluid temperature and the pressure drop along the nozzle for seven different conditions. The seven conditions differ among them by the length of the

*Corresponding author: raul.ochoterena@chalmers.se

Table 1. Selected properties of water as function of temperature.

$T\ [°C]$	$\rho\ [kg/m^3]$	$\gamma\ [mN/m]$	$\mu\ [mPa \cdot s]$	$P_v\ [kPa]$
22	997	72.8	1.00	2.34
40	992	69.9	0.65	7.38
60	983	66.9	0.47	19.9
80	972	64.0	0.36	47.4

cavitation cloud measured from the inlet of the contraction zone of the nozzle, referred here as cavitation length (CA). The first experimental condition is set to have no cavitation inside the nozzle, achieving this by reducing the pressure in the nozzle after the slightest inception of cavitation is noticed. In the following conditions the cavitation length ranges from the inception of cavitation until the cavitation length is almost equal to the nozzle length. In the last condition a hydraulic flip is induced by moderately increasing the pressure in the nozzle after the farthest downstream border of the cavitation cloud reached the outlet of the nozzle. This transforms the atomising spray into a non-atomising jet.

The cone angle was determined from a series of photographs that were captured with a high speed camera using back light illumination and digitally processed using an edge detection algorithm.

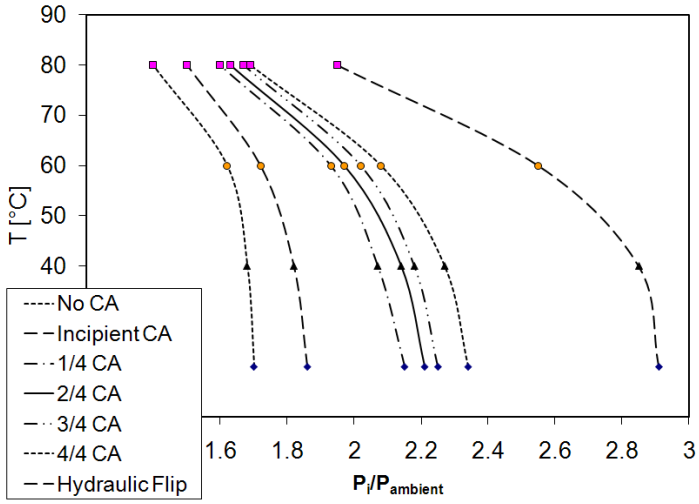

Figure 3. Experimental test matrix.

Results and discussion

Flow measurements

Volumetric flow measurements as function of the pressure inside the nozzle, injecting water at ambient temperature and corresponding to the sharp inlet nozzle, are presented in Figure 4. It is observed that the flow increases proportional to the square root of the pressure drop along the nozzle until the cavitation length is almost equal to the nozzle length. A further increase in the pressure inside the nozzle leads to a hydraulic flip and a reduction in the volumetric flow rate through the nozzle.

Volumetric flow measurements for every point contained on the test matrix (Fig. 3) corresponding to the sharp and blunt inlet nozzles (Fig. 2) are plotted in Figure 5. It is possible to observe that, for the range of pressure that was studied in this work, the volumetric flow rate through the blunt inlet nozzle increases proportionally to the square root of the differential pressure across the nozzle. Moreover, than the sharp inlet nozzle has a lower flow rate, compared to the blunt inlet nozzle, for the same differential pressure; however and as expected, a substantial

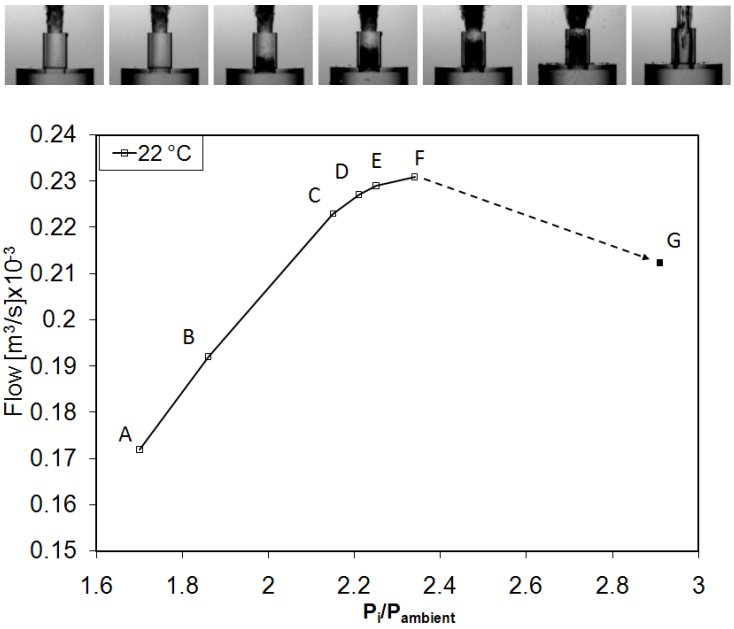

Figure 4. Flow measurements as a function of pressure at ambient temperature for the sharp inlet nozzle. A: no cavitation, B: nncipient cavitation, C: CA length equal to one fourth the nozzle length, D: CA length equal to two quarters of the nozzle length, E: CA length equal to three quarters of the nozzle length, F: CA length almost equal to the nozzle length, G: hydraulic flip.

reduction in the flow is noticed after the development of the hydraulic flip. Additionally, the flow rate reduction caused by the development of the hydraulic flip is substantially smaller for water at high temperatures than for water at low temperatures.

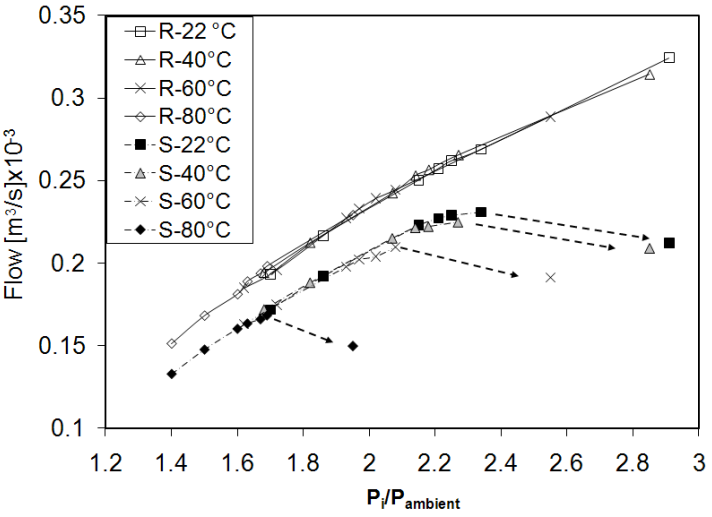

Figure 5. Flow measurements as a function of pressure at four different temperatures for the sharp inlet nozzle (S) and for the blunt inlet nozzle (R).

The discharge coefficient ($Cd = \dot{m}/A_0\sqrt{2\rho\Delta P}$) as function of pressure inside the sharp inlet nozzle is shown in Figure 6. It is observable that Cd diminishes from the inception of cavitation and reaches a relative minimum after the occurrence of the hydraulic flip. It is worth to highlight that equivalent lengths of the cavitation cloud inside the nozzle (CA) lead to almost equal values of the discharge coefficient (Cd) regardless of the temperature or the velocity of the fluid.

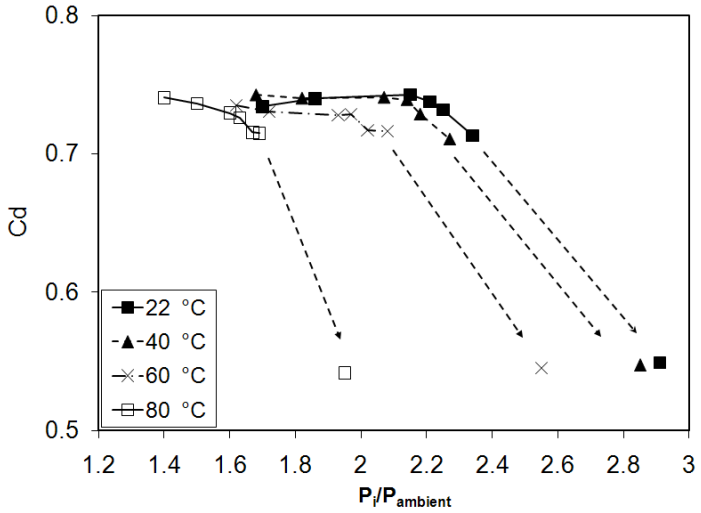

Figure 6. Discharge coefficient as function of pressure for the sharp inlet nozzle. The points correspond to the points presented in the test matrix (Fig. 3).

Reynolds number

Reynolds number ($Re = \rho U_\infty L/\mu$) where L is the nozzle diameter, was calculated for the points considered in the test matrix (Fig. 3). Plots of the Reynolds number against pressure inside the nozzle are shown in Figure 7 and Figure 8, for the sharp and blunt inlet nozzles respectively.

In these plots it is noticed that the slope of the curve increases for higher temperatures, also that the Re difference between consecutive temperatures, for the same cavitation length, appears to be consistent, except for the difference in the Reynolds number between the $60°C$ and $80°C$ cases, where the difference is considerably smaller than for lower temperatures.

For the sharp inlet nozzle, Re reaches a plateau where cavitation dominates the flow inside the nozzle, after the hydraulic flip occurs, Reynolds drops. The Reynolds difference between the penultimate and last flow conditions, where cavitation length is almost equal to the nozzle length and after the hydraulic flip occurs, is much higher for the high temperature cases than for low temperatures cases.

For the blunt inlet nozzle, Re increases monotonically proportional to the square root of the pressure drop due to the fact that cavitation is not present the inner nozzle flow.

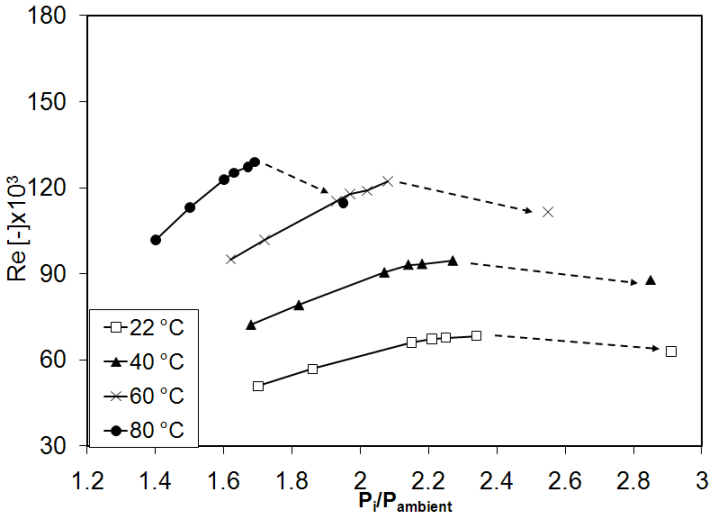

Figure 7. Reynolds number as function of pressure for four different temperatures for the sharp inlet nozzle.

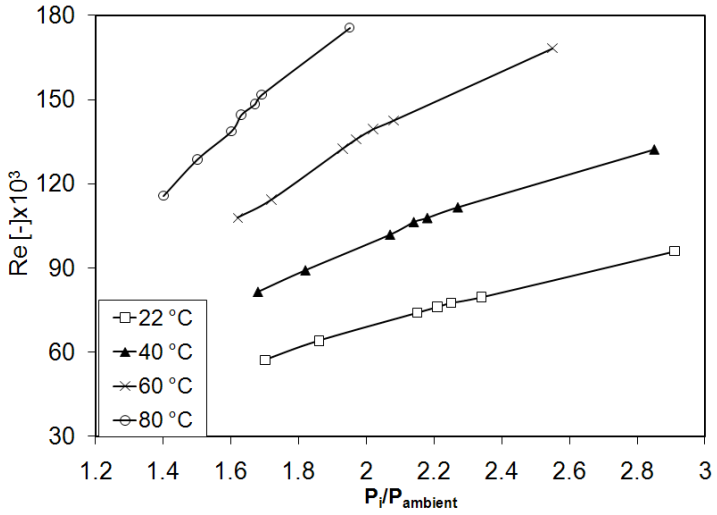

Figure 8. Reynolds number as function of pressure for four different temperatures for the blunt inlet nozzle.

Cavitation number

Plots of the Cavitation Number $(CN)^*$ against the pressure inside the nozzle, and for the points considered in the test matrix (Fig. 3), are shown in Figure 9 and Figure 10 for the sharp and blunt inlet nozzles respectively.

Large values of the CN indicate single-phase liquid flow, whether small values of CN indicate the possibility of the occurrence of cavitation. For the sharp inlet nozzle case it can be noticed that the Cavitation Number diminishes as the pressure inside the nozzle increases until the Cavitation Number reaches a value close to unity occurring when cavitation almost dominates the flow inside the nozzle. A further increase in the pressure inside the nozzle leads to the appearance of the hydraulic flip. After the hydraulic flip occurs the Cavitation Number increases due to an increase in the pressure drop across the nozzle and to a reduction of the flow rate.

The blunt inlet nozzle case (Fig. 10), which presents no cavitation inside the nozzle neither atomisation, shows a continuous reduction on the Cavitation Number as the pressure drop across the nozzle increases; however, this is not linear. Even though the Cavitation Number can have values lower than unity, no cavitation is present through the contraction zone of the nozzle for the studied pressure interval.

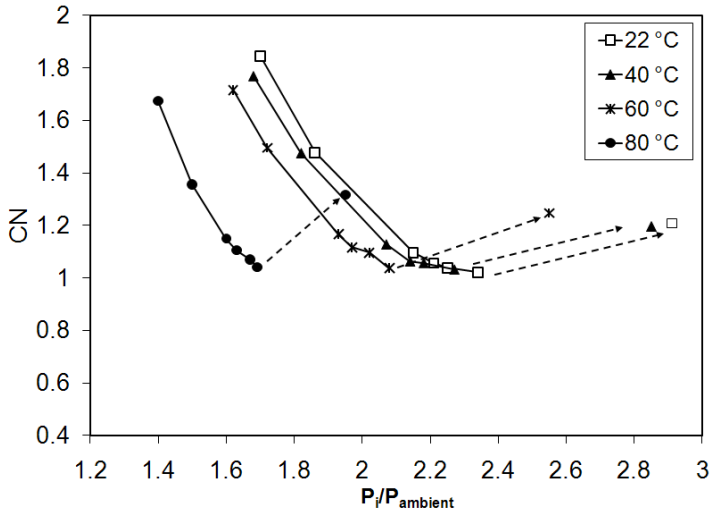

Figure 9. Cavitation number as function of pressure for four different temperatures for the sharp inlet nozzle.

$^*CN = \dfrac{P_\infty - P_v(T\infty)}{\frac{1}{2}\rho U_\infty^2}$

T_∞, P_∞ and U_∞ are the reference temperature, the pressure and velocity of the flow, respectively.

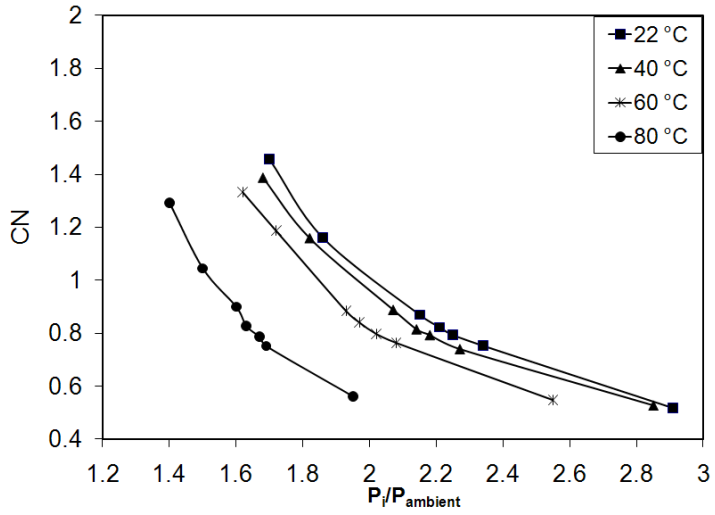

Figure 10. Cavitation number as function of pressure for four different temperatures for the blunt inlet nozzle.

Weber number

Weber number ($We = \rho U_\infty^2 L/\gamma(T_\infty)$) was calculated as function of the Reynolds number for the points considered in the test matrix. Plots relating Weber and Reynolds numbers are presented in Figure 9 and Figure 10, for the sharp and blunt inlet nozzles respectively. The ratio between Weber and Reynolds numbers relates inertial and viscous effects against surface tension forces being the slope of the plots equal to $2U_m\mu/\gamma$, where U_m is the mean velocity of the flow between points.

In both cases, sharp and blunt inlet nozzles, the slope of the curves decreases considerably as temperature increases. This change on the slope between Weber and Reynolds numbers emphasises the strong influence that the fluid temperature has on the dynamic viscosity of water. It is observed that Weber number is almost constant between ambient and the consecutive temperature for the points which correspond to a similar degree of cavitation, meanwhile Reynolds number is almost constant between the penultimate and the highest temperature for the points which correspond to the same length of cavitation.

Although the plots are not linear since the velocity of the flow is affected by cavitation, the points for each temperature are contained in the same plot even after the hydraulic flip occurs.

It was decided to present these plots rather than only calculations of the Ohnesorge number (Oh[†]) since this one does not include the velocity of the flow and therefore it is constant for each of the studied temperatures regardless of the flow rate, nozzle geometry or CA. The values for the studied temperatures are $Oh_{22^\circ C} = 16.15 \times 10^{-4}$, $Oh_{40^\circ C} = 11.59 \times 10^{-4}$, $Oh_{60^\circ C} = 8.53 \times 10^{-4}$ and $Oh_{80^\circ C} = 6.63 \times 10^{-4}$. It is clear that surface tension effects become dominant and viscous effects loose relevance as the fluid temperature is risen.

Cone angle

Cone angle was measured from the images captured with a high speed camera using back light illumination and a derivative edge detection method for detecting the borders of the spray. Measurements were conducted using the sharp inlet nozzle. Every measurement point represents the average data of one hundred measurements. Measurements were performed at three different distances downstream the nozzle exit, one, five and fifteen nozzle diameters respectively. Results of these measurements are presented on Figure 13 and Figure 14.

Figure 13 shows measurements of the spray cone angle against the pressure inside the nozzle. It can be observed that the cone angle decreases as the distance from the nozzle exit increases. It is also noticed that the cone angle increases abruptly from the point where cavitation inception is present, further on, the cone angle increases until it reaches a maximum point where the cavitation length is almost equal to the nozzle length, a further increase on pressure leads to the hydraulic flip where a non-atomising jet is produced.

Figure 14 shows measurements of the spray cone angle against liquid temperature measured at three different distances downstream the nozzle exit, one, five and fifteen diameters. Figures show that maintaining cavitation length inside the nozzle as constant, even with an increase on the fluid temperature, produces a similar degree

[†] $Oh = \mu/\sqrt{\rho\gamma(T_\infty)L}$

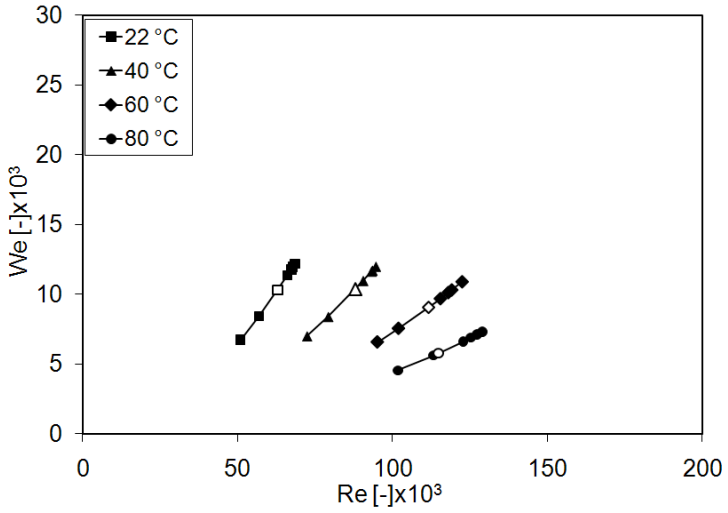

Figure 11. Weber number as function of Reynolds for four different temperatures for the sharp inlet nozzle. The not-filled markers correspond to values after the hydraulic flip occurs.

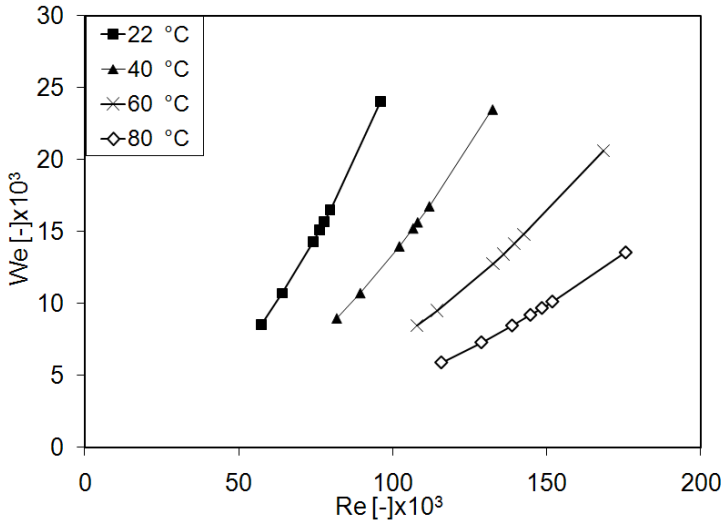

Figure 12. Weber number as function of Reynolds for four different temperatures for the blunt inlet nozzle.

of atomisation. It can be clearly seen that an increase on cavitation inside the nozzle leads to a higher degree of atomisation.

Figure 15 depicts a series of photographs for the sharp inlet nozzle for four different liquid temperatures and different cavitation lengths. Pictures show the different test points contained on the test matrix (Fig. 3).

In general, it is possible to observe that similar lengths of cavitation lead to sprays which are comparable among them. Furthermore, that maintaining the cavitation length inside the nozzle as constant leads to similar degree of atomisation regardless of fluid temperature, pressure drop or flow rate across the nozzle. It is shown that an increase in cavitation inside the nozzle leads to higher cone angles and consequently into a higher degree of atomisation.

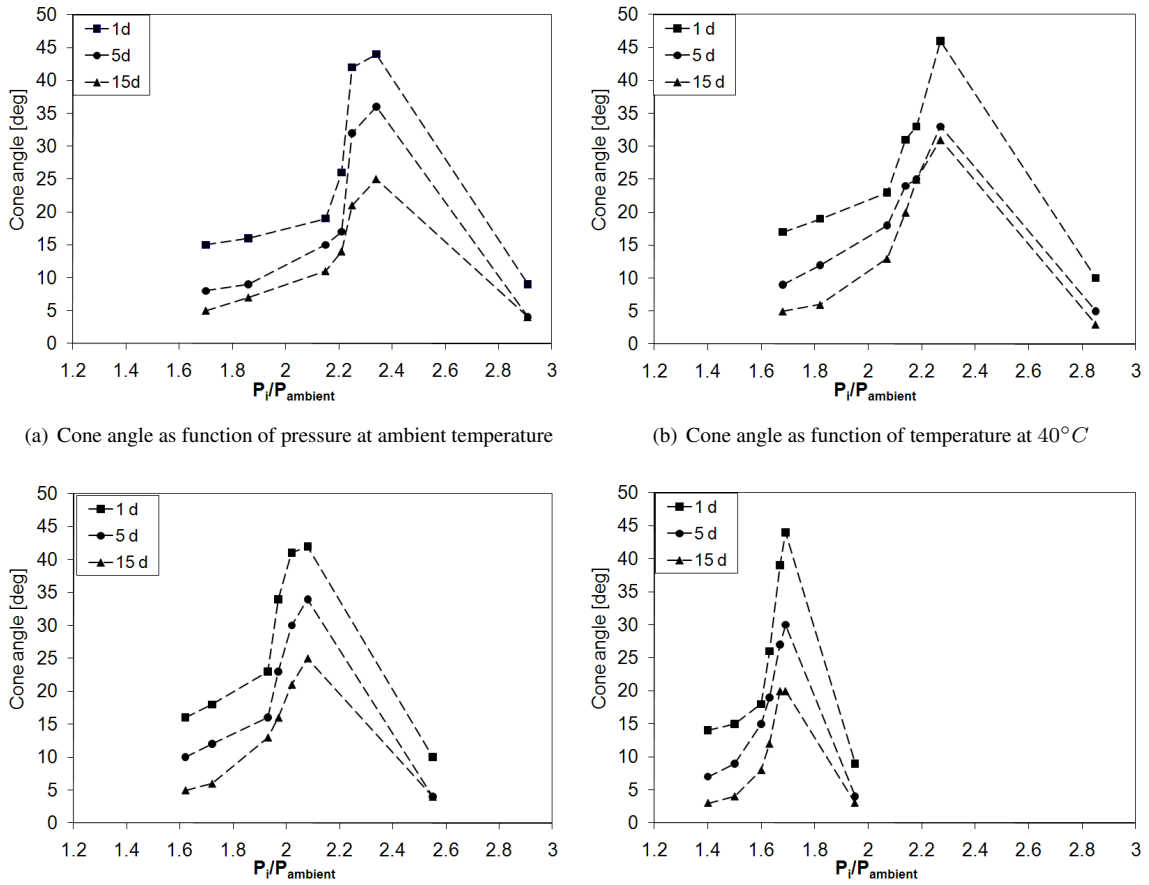

(a) Cone angle as function of pressure at ambient temperature

(b) Cone angle as function of temperature at $40°C$

(c) Cone angle as function of temperature at $60°C$

(d) Cone angle as function of temperature at $80°C$

Figure 13. Cone angle measurements for four different temperatures for the sharp inlet nozzle measured at one diameter (1d), five diameters (5d) and fifteen diameters (15d) downstream the nozzle exit.

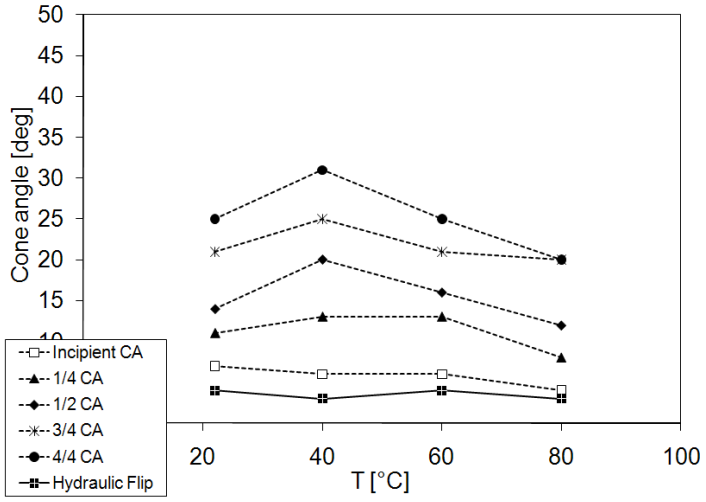

(a) Cone angle as function of temperature at fifteen diameters downstream the nozzle exit

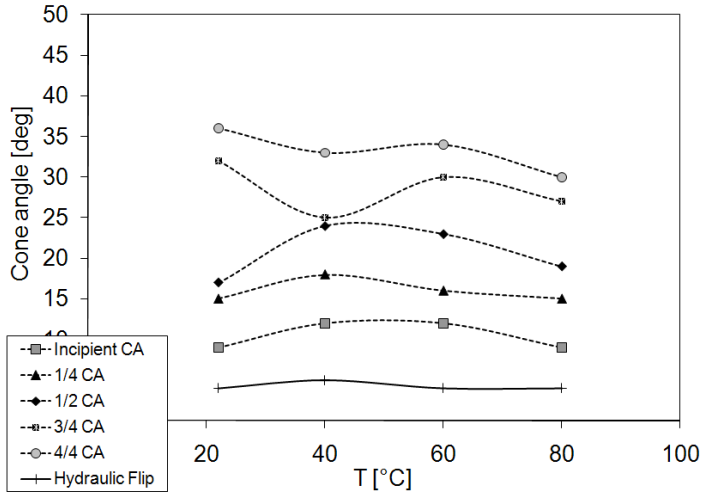

(b) Cone angle as function of temperature at five diameters downstream the nozzle exit

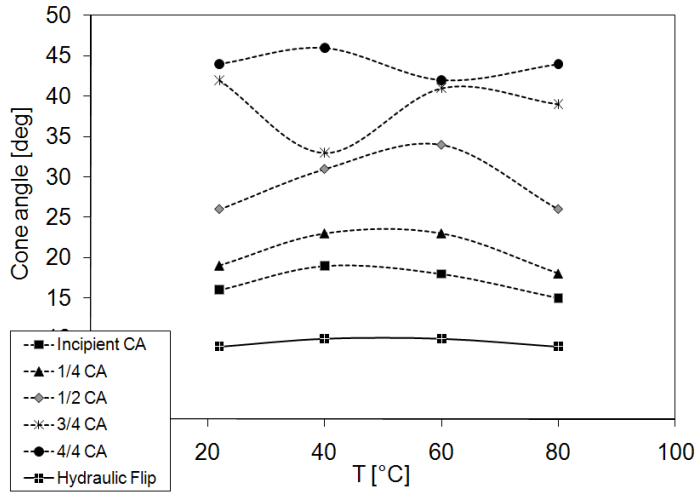

(c) Cone angle as function of temperature at one diameter downstream the nozzle exit

Figure 14. Cone angle measurements measured as function of temperature

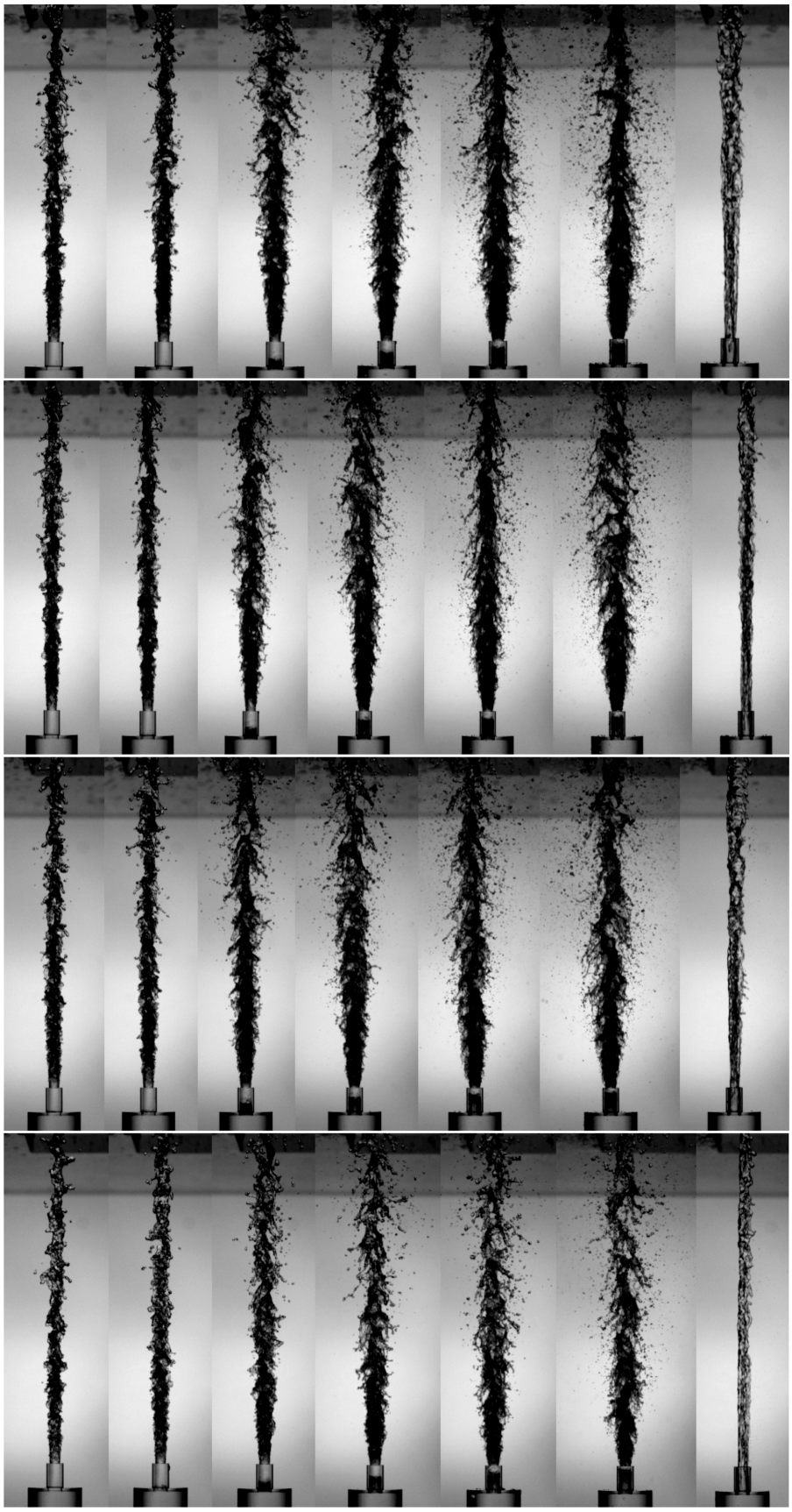

Figure 15. Photograph series for the sharp inlet nozzle for different cavitation lengths at four different temperatures; $20^{\circ}C$, $40^{\circ}C$, $60^{\circ}C$ and $80^{\circ}C$ from top. From the left hand side: A-no cavitation, B-incipient cavitation, C-CA length equal to one fourth the nozzle length, D-CA length equal to two quarters of the nozzle length, E-CA length equal to three quarters of the nozzle length, F-CA length almost equal to the nozzle length, G-Hydraulic flip

Conclusions

Experiments to disclose the influence that cavitation has on atomisation were conducted, promoting cavitation inside the nozzle by means of modifying the temperature and consequently the vapour pressure of the injected liquid. Results indicate that, in systems where the effects of the aerodynamic forces are small compared to the internal flow effects, cavitation length can be correlated to atomisation regardless of the fluid temperature, flow regime or pressure drop across the nozzle. However, it was not possible to separate the solely effect that cavitation or turbulence have on atomisation due to the fact that these experiments were conducted at high Reynolds numbers where turbulence is undoubtedly present.

Acknowledgements

Financial support from the Combustion Engine Research Centre (CERC) at Chalmers is greatly appreciated.

References

[1] Lamb, H., “Hydrodynamics.", 6th Edition. Dover, New York., (1932).
[2] Reitz R.D. and Bracco F.V., “Mechanism of Break-up of Round Liquid jets.", The Encyclopaedia of Fluid Mechanics., ed. Cheremisnoff, **Vol. 3**, 233-243 (1986).
[3] Bergwerk W., “Flow pattern in diesel nozzle spray holes.", Proc. Inst. Mech. Eng., **173:25**, 655-660 (1959).
[4] von Berg E., Grief D., Tatschl R., Winklhofer E., Ganippa L.C. “Primary break-up model for diesel jets based on locally resolved flow properties in the injection hole." ILASS-Europe, 9-11 September, 2002, Zaragoza, Spain.
[5] Soteriou C., Andrews R., and Smith M.,“Further Studies of Cavitation and Atomisation in Diesel Injection”, SAE Paper 1999-01-1486.
[6] Ochoterena R., and Anderssson S., “Flow in Nozzles and its Influence on Spray Behaviour”, ILASS EUROPE, Nottingham, United Kingdom, 6-8 September, 2004.
[7] Brennen C. E., “Cavitation and Bubble Dynamics”, 1st Edition. Oxford University Press., (1995).
[8] P. Li and M. Vera-Hernández, “Influence of cavitation on atomisation of low pressure, up-scaled, transparent nozzles´´, Master Thesis, Chalmers University of Technology, ISSN 1652-8557, Göteborg, Sweden, (2006).